A Role for RIC-8 (Synembryn) and GOA-1 ($G_o\alpha$) in Regulating a Subset of Centrosome Movements During Early Embryogenesis in *Caenorhabditis elegans*

Kenneth G. Miller and James B. Rand

Program in Molecular and Cell Biology, Oklahoma Medical Research Foundation, Oklahoma City, Oklahoma 73104

Manuscript received July 7, 2000
Accepted for publication August 25, 2000

ABSTRACT

RIC-8 (synembryn) and GOA-1 ($G_o\alpha$) are key components of a signaling network that regulates neurotransmitter secretion in *Caenorhabditis elegans*. Here we show that *ric-8* and *goa-1* reduction of function mutants exhibit partial embryonic lethality. Through Nomarski analysis we show that *goa-1* and *ric-8* mutant embryos exhibit defects in multiple events that involve centrosomes, including one-cell posterior centrosome rocking, P_1 centrosome flattening, mitotic spindle alignment, and nuclear migration. In *ric-8* reduction of function backgrounds, the embryonic lethality, spindle misalignments and delayed nuclear migration are strongly enhanced by a 50% reduction in maternal *goa-1* gene dosage. Several other microfilament- and microtubule-mediated events, as well as overall embryonic polarity, appear unperturbed in the mutants. In addition, our results suggest that RIC-8 and GOA-1 do not have roles in centrosome replication, in the diametric movements of daughter centrosomes along the nuclear membrane, or in the extension of microtubules from centrosomes. Through immunostaining we show that GOA-1 ($G_o\alpha$) localizes to cell cortices as well as near centrosomes. Our results demonstrate that two components of a neuronal signal transduction pathway also play a role in centrosome movements during early embryogenesis.

THE proper movement and positioning of centrosomes is an essential feature of development because it determines the alignment of the mitotic spindle, which in turn determines the cleavage plane at cytokinesis (reviewed by Rappaport 1996). In early *Caenorhabditis elegans* embryos, the mitotic spindle of each cell assumes a stereotypical alignment that ensures that the cells have a fixed position with respect to each other (Sulston *et al.* 1983). Correct spindle orientation is especially important for asymmetric cell divisions, since the cleavage plane must ensure that localized determinants are segregated to only one of the two daughter cells (see Guo and Kemphues 1996; White and Strome 1996; Knoblich 1997; Bowerman 1998; Hawkins and Garriga 1998; Lu *et al.* 1998; for reviews).

Centrosomes also mediate nuclear migrations in a variety of cells and organisms. The recently characterized *C. elegans unc-84* gene, mutants of which have nuclear migration defects in larval and adult cells, encodes a protein with similarity to a *Schizosaccharomyces pombe* spindle pole body protein (the yeast spindle pole body is analogous to the centrosome; Malone *et al.* 1999). In Drosophila embryos in which nuclear division is inhibited, the centrosomes continue to replicate and migrate normally without their nuclei (Raff and Glover 1989). Finally, in fungal cells, nuclear migration also appears to be mediated by the spindle pole body (reviewed in Morris *et al.* 1995).

Studies in *C. elegans* and in other organisms have begun to define the machinery that mediates centrosome movement during mitotic spindle alignment and nuclear migration. In brief, these studies indicate that centrosomes are pulled, via microtubules, by the motor protein dynein, which is anchored to dynactin complexes at discrete sites on or near the plasma membrane (dynactin is a complex of several different proteins; Hyman 1989; see Morris *et al.* 1995; Skop and White 1998; Heil-Chapdelaine *et al.* 1999; Karki and Holzbaur 1999 for additional references). A second mechanism for spindle positioning, which is redundant with the dynein/dynactin complex, has also been identified in budding yeast (see Lee *et al.* 2000 for references).

Other studies have begun to identify both intrinsic and extrinsic signals that regulate mitotic spindle alignment. In the Drosophila neuroblast, spindle alignment appears to be regulated by the activities of Inscuteable and the PDZ-domain-containing protein Bazooka (reviewed in Jan and Jan 2000). In *C. elegans*, the PAR group of proteins, including the Bazooka homolog PAR-3, is crucial for establishing the polarity of early embryonic cells. All of the PAR proteins, except PAR-1 and PAR-4, regulate mitotic spindle alignment in specific cells by one or more cell intrinsic mechanisms (Strome *et al.* 1995; Guo and Kemphues 1996; Bowerman 1998). In contrast, extrinsic signals (sent from the P_2 cell) regulate the mitotic spindle orientation of the EMS cell (Goldstein 1995). A subset of Wnt path-

Corresponding author: James B. Rand, Program in Molecular and Cell Biology, Oklahoma Medical Research Foundation, Oklahoma City, OK 73104. E-mail: randj@omrf.ouhsc.edu

way components mediates this alignment (Schlesinger *et al.* 1999). Several Wnt pathway components (Frizzled, Dishevelled, Flamingo) also regulate mitotic spindle alignment in the Drosophila sensory organ precursor cells (reviewed in Jan and Jan 2000).

It is not yet clear, however, how developmental signals regulate the position of the centrosomes. The finding that GPB-1 (Gβ) is required for mitotic spindle alignment in early *C. elegans* embryos suggests that one or more heterotrimeric G proteins are required for centrosome positioning (Zwaal *et al.* 1996). This is supported by a recent investigation of mitotic spindle alignment in the Drosophila neuroblast in which the novel protein Partner of Inscuteable (Pins) and a Gα subunit (identified as either $G_o\alpha$ or $G_i\alpha$) were found to bind specifically to the functional domain of Inscuteable (Schaefer *et al.* 2000). However, although Pins is required for proper mitotic spindle alignment (Schaefer *et al.* 2000; Yu *et al.* 2000), a requirement for the associated Gα protein, or indeed any Gα protein, in mitotic spindle alignment has not yet been demonstrated. Furthermore, no signal transduction protein that regulates nuclear migrations in any organism has been identified.

We recently identified RIC-8 (synembryn) as a novel 63-kD cytoplasmic protein that is required for EGL-30 ($G_q\alpha$) pathway activity in the *C. elegans* nervous system and is conserved in vertebrates (Miller *et al.* 2000). RIC-8's function in the nervous system is also closely associated with the G protein GOA-1 ($G_o\alpha$), which negatively regulates EGL-30 ($G_q\alpha$) signaling (Hajdu-Cronin *et al.* 1999; Miller *et al.* 1999). RIC-8 and GOA-1 are key components of a network of proteins, known as the $G_o\alpha$-$G_q\alpha$ signaling network, that regulates neurotransmitter secretion in *C. elegans* by controlling the production and consumption of diacylglycerol (DAG; Hajdu-Cronin *et al.* 1999; Lackner *et al.* 1999; Miller *et al.* 1999, 2000; Nurrish *et al.* 1999). We now report that RIC-8 and GOA-1, in addition to their roles in the adult nervous system, also play a role in mitotic spindle alignment, nuclear migration, and other centrosome-mediated events during early embryogenesis in *C. elegans*. Through immunostaining we show that, in embryos, the G protein GOA-1 ($G_o\alpha$) localizes to cell cortices as well as near centrosomes.

MATERIALS AND METHODS

General methods and strains: Worms were cultured using standard methods (Brenner 1974). Wild-type worms were *C. elegans* variety Bristol, strain N2. The following *C. elegans* mutant strains were used in this work:

Single mutants: MT2426 *goa-1(n1134)I*, RM2225 *goa-1(pk62)I*, RM2226 *goa-1(n363)I*, RM1702 *ric-8(md303)IV*, RM2209 *ric-8(md1909)IV*, RM2235 *ric-8(md1712 md303)IV*.

Double mutants: *goa-1(n363)/+I*; *ric-8(md1909)IV*, *goa-1(pk62)/+I*; *ric-8(md303)IV*, *goa-1(n1134)/+I*; *ric-8(md303)IV*, *goa-1(n1134)/+I*; *ric-8(md1909)IV*, RM2218 *ric-8(md303)IV*; *dgk-1(sy428)X*.

Double mutant strain construction and verification: The *ric-8* reduction-of-function mutants and the *ric-8(md1712 md303)* intragenic revertant are described in Miller *et al.* (2000). *dgk-1(sy428)* and *goa-1(n363)* are loss-of-function or null alleles (Ségalat *et al.* 1995; Hajdu-Cronin *et al.* 1999). *dgk-1 (sy428)* contains an early stop codon in the coding sequences of *dgk-1* (S. Nurrish and J. Kaplan, personal communication). *goa-1(pk62)* and *goa-1(n1134)* are strong reduction-of-function alleles (Ségalat *et al.* 1995; Mendel *et al.* 1995).

Double mutants were constructed using standard genetic methods, without additional marker mutations. Homozygosity of *ric-8(md303)* in double mutants was confirmed by sequencing amplified genomic DNA from double-mutant strains. Homozygosity of *dgk-1* alleles (X linked) was confirmed by noncomplementation tests. The presence of a single copy of *goa-1(n1134)* in *goa-1(n1134)/+; ric-8(md303)/ric-8(md303)* was confirmed by PCR amplification and sequencing of the relevant region of the *goa-1* gene. To identify parental animals of the genotype *goa-1/+; ric-8/ric-8* for observation of their progeny, *ric-8* mutants (identified by their Egl, sluggish, and reduced body flexion phenotypes) were selected from the progeny of *goa-1/+; ric-8/+* animals. Two-thirds of these *ric-8* mutants carry *goa-1/+* and segregate mostly dead embryos.

Embryonic lethality counts: For all homozygous strains, as well as *goa-1/+* heterozygous strains, three populations of day 1 adults were placed on culture plates and allowed to lay eggs for 24 hr at 20°. Parental animals were then removed, and the plates were incubated 24 hr at 20° to allow viable embryos to hatch. The number of animals per population was chosen so that each population yielded ~300 eggs during the 24-hr period. Larva and unhatched eggs were then counted against a gridded background. To quantify embryonic lethality in the progeny of *goa-1/+; ric-8/ric-8*, *ric-8* mutants were cloned from the progeny of *goa-1/+; ric-8/+*. Parental animals of the genotype *goa-1/+; ric-8/ric-8* were identified by their production of nearly 100% dead eggs. The progeny of five to seven such animals were scored for embryonic lethality.

To test for zygotic rescue of *ric-8(md303)*, N2 males were mated to *ric-8(md303)* young adults. Parental animals were removed after 24 hr, and plates were assayed 24 hr later. Four individual matings were quantified in this way. Self-progeny, which were distinguished from cross-progeny by their adult mutant phenotypes, were counted 4 days after the matings were set up and ranged from 10 to 25% of the total progeny.

To test for maternal rescue of *ric-8(md303)*, wild-type males were mated to *ric-8(md303)* hermaphrodites, and wild-type hermaphrodite L4-stage progeny of the cross were picked to culture plates (six L4 cross progeny per plate). These cross-progeny were allowed to develop to adulthood and lay eggs for 32 hr at 20° and then were killed. After further incubation of the plates at 20° for 18 hr (to allow all viable eggs to hatch) the plates were scored for unhatched eggs.

Observations of early embryonic development: We obtained embryos for observation of early development based on the protocols of Sulston and Hodgkin (1988) and Zwaal *et al.* (1996). Wild-type or mutant adult hermaphrodites were cut in half in egg salts [5 mm HEPES (pH 7.2), 110 mm NaCl, 4 mm KCl, 5 mm $MgCl_2$] on a glass microscope slide. Fertilized eggs and embryos were extruded by applying pressure with a wire pick. Recently fertilized eggs were identified by the presence of anterior membrane contractions and transferred using a mouth pipette to a poly-L-lysine-coated coverslip. The embryos were then gently mounted on a freshly made 2% agar pad on a microscope slide, and the edges of the coverslip were sealed with petroleum jelly. Embryonic development was viewed at 22° using Nomarksi optics with a Zeiss Plan-NEOFLUOR ×100, 1.3 N.A., polarized oil immersion objective (Carl Zeiss, Thornwood, NY) with a green filter to block heat and improve

contrast. Times of key events relative to pronuclear fusion and completion of the first cell division were noted. Embryos were photographed at regular intervals using Kodak Tmax 400 ASA film. Centrosome positions and spindle orientations were noted at prometaphase and metaphase.

Immunostaining: The GOA-1 antibody (gift of Michael Koelle) is a rabbit polyclonal raised against full-length, His-tagged, bacterially expressed GOA-1. The antiserum was affinity purified against the recombinant protein.

Whole mounts of *C. elegans* adults were prepared for antibody staining as described previously, using methanol/acetone fixation (Duerr *et al.* 1999). Embryos were prepared and fixed for antibody staining as described previously, using methanol/acetone fixation (Zwaal *et al.* 1996). All primary antibody incubations were at room temperature for overnight. The GOA-1 antibody (gift of Michael Koelle) was used at a 1/100 dilution. The rat antitubulin monoclonal antibody (YL1/2; Serotec) was used at 1/10. PGL-1 antibody (gift of Susan Strome) was used at 1/6700. CHA-1 monoclonal antibody supernatants were a gift of Janet Duerr and were used undiluted. Secondary antibodies (adsorbed against 4% formaldehyde-fixed worms to remove antibodies to nematode proteins) were donkey anti-rabbit antibodies (Jackson Immuno Research) coupled to Alexa 488 dye (Molecular Probes, Eugene, OR; to visualize GOA-1 and PGL-1) and donkey anti-rat antibodies coupled to Cy3 (to visualize tubulin and CHA-1). Secondary antibody incubations were for 2 hr at room temperature for embryos and 4 hr at room temperature for adults. 4′6-Diamidino-2-phenylindole (DAPI; 4 μg/ml) was included in the mounting medium to visualize DNA. Specimens were viewed using a Leica ×100 Plan APO 1.4 N.A. oil immersion lens, and images were collected using the Leica TCS NT Confocal system and accompanying software. Images were further processed using Adobe Photoshop 5.0.

RESULTS

GOA-1 ($G_o\alpha$) interacts with RIC-8 during embryogenesis: In previous studies, we found that *ric-8* reduction-of-function mutations result in strong neuronal phenotypes including decreased locomotion, egg laying, and body flexion, as well as resistance to inhibitors of cholinesterase (Miller *et al.* 1996, 2000). In this study, we observed that *ric-8(md303)* reduction of function mutants also exhibit 29% embryonic lethality. A weaker mutant, *ric-8(md1909)*, exhibits 15% embryonic lethality. This lethality is the result of mutations in the *ric-8* gene because the intragenic suppressor mutant *ric-8(md1712 md303)* exhibits wild-type levels of embryonic survival. This suppressor contains a second-site mutation that is eight amino acids upstream of the original missense *md303* mutation (Miller *et al.* 2000).

While investigating the relationship of RIC-8 to the $G_o\alpha$-$G_q\alpha$ signaling network, we observed that the embryonic lethality of *ric-8* mutants was enhanced to nearly 100% in embryos derived from a *goa-1/+; ric-8/ric-8* parent. We observed this enhanced embryonic lethality in six different allele combinations of *goa-1*; *ric-8* double mutants; results from four of these combinations are shown in Table 1. The *goa-1* mutants used for this experiment are reduction- or loss-of-function mutants, and embryos born to *goa-1/+* parents in *ric-8(+)* backgrounds exhibit wild-type levels of embryonic survival (Table 1). The fact that a 50% decrease in maternal *goa-1* gene dosage cannot support embryogenesis in backgrounds with reduced RIC-8 function suggests that GOA-1 and RIC-8 function in the same process or pathway in one or more events during early embryogenesis.

TABLE 1

Genetic interactions between *goa-1* and *ric-8* during embryogenesis

Genotype of parent	% embryonic or early larval lethal among progeny[a]	Progeny counted[b]
Wild type (N2)	0.93 ± 0.74	885
ric-8(md303)	29 ± 2.3	952
ric-8(md303)/+	1.4 ± 0.73	684
ric-8(md1712 md303)	0.13 ± 0.13	683
ric-8(md1909)	15 ± 1.7	968
egl-30(ad805)	0.0 ± 0.0	399
goa-1(n1134)	5.1 ± 1.3	1081
goa-1(n363)	11 ± 1.4	828
goa-1(pk62)	22 ± 6.3	1055
goa-1(pk62)/goa-1(n363)	11 ± 0.91	1827
goa-1(pk62)/+	0.67 ± 0.34	1108
goa-1(n1134)/+	0.32 ± 0.18	630
goa-1(pk62)/+; ric-8(md303)	98 ± 0.92[c]	219
goa-1(n1134)/+; ric-8(md1909)	100 ± 0.27[c]	509
goa-1(n1134)/+; ric-8(md303)	96 ± 1.4[c]	385
goa-1(n363)/+; ric-8(md1909)	97 ± 1.9[c]	679
ric-8(md303); dgk-1(sy428)	28 ± 2.1	1036

[a] Mean ± standard error.

[b] Progeny were equally divided among at least three independent populations. All progeny counts are from broods produced within the first 24 hr of adulthood.

[c] <5% of this number represents early larval lethality, while >95% of this number represents embryonic lethality.

These results led us to determine if homozygous *goa-1* reduction- and loss-of-function mutants exhibit embryonic lethality. Indeed, we observed 5 and 22% embryonic lethality in two *goa-1* reduction-of-function mutants and 11% embryonic lethality in the putative null mutant *n363*. This embryonic lethality is likely caused by mutations at the *goa-1* locus, as opposed to other linked mutations, because embryos derived from *goa-1(pk62)/goa-1(n363)* animals also exhibited 11% embryonic lethality (Table 1).

Although previous studies showed that GOA-1 regulates the EGL-30 ($G_q\alpha$) pathway in the adult nervous system (Hajdu-Cronin *et al.* 1999; Miller *et al.* 1999), we observed no embryonic lethality in strong reduction-of-function *egl-30* mutants (Table 1). In addition, a separate study found that putative *egl-30* null mutants arrest

at larval stages (Brundage *et al.* 1996). EGL-30, therefore, appears not to be required to complete embryogenesis. A recent study found that loss of DGK-1 (diacylglycerol kinase) strongly suppresses the neuronal phenotypes of *ric-8* mutants (Miller *et al.* 2000). However, we observed that the embryonic lethality of *ric-8* mutants is the same whether or not DGK-1 is present (Table 1). Although we have not ruled out the involvement of other components of the $G_o\alpha$-$G_q\alpha$ signaling network in embryogenesis, these findings suggest that EGL-30 and DGK-1 are not required to complete embryogenesis.

RIC-8 functions during early embryogenesis: We used Nomarski optics to examine the terminal phenotype of *ric-8(md303)* embryos that failed to complete embryogenesis as well as the terminal phenotype of embryos derived from *goa-1/+; ric-8/ric-8*. We found that these embryos were essentially composed of a disorganized mass of tissues. Within this mass, however, we observed fully differentiated cell types including body wall muscle, pharynx, gut, and hypodermis. The presence of movement in the muscle tissue of these embryos confirmed that at least some of these cells were alive and functional at late stages in embryogenesis (data not shown).

To investigate when RIC-8 is required during embryogenesis, we tested if maternal expression of *ric-8* is sufficient to rescue the embryonic lethality of *ric-8* mutants by scoring embryonic lethality in the progeny of *ric-8(md303)/+* animals. We observed a 1.4 ± 0.7% rate of embryonic lethality in the progeny of *ric-8(md303)/+* animals (Table 1). If *ric-8* expression were not required maternally, then the rate of embryonic lethality in these animals should be ~7%, since 25% of the progeny will be homozygous for *ric-8* and 29% of *ric-8(md303)* homozygotes exhibit embryonic lethality. The observed 1.4% rate of embryonic lethality suggests that maternal expression from a single *ric-8* (+) chromosome is sufficient to rescue most, but apparently not all, of the embryonic lethality in *ric-8* homozygotes.

To determine if embryonic (zygotic) expression of *ric-8* is sufficient to rescue *ric-8* mutants, we mated wild-type males to *ric-8(md303)* hermaphrodites. We observed that the rate of embryonic lethality in the resulting progeny is 12 ± 3% (mean ± standard error; 1128 progeny divided among 3 independent populations), which is ~40% of the rate observed in *ric-8(md303)*. Therefore, embryonic expression of *ric-8* is not sufficient to fully rescue *ric-8(md303)* mutants. Although we do not yet know when *ric-8* is first transcribed in the embryo, a previous study showed that some embryonic RNAs are transcribed in somatic blastomeres as early as the four-cell stage (Seydoux *et al.* 1996).

In summary, these experiments suggest that *ric-8* is expressed maternally and thus acts during early embryogenesis. *ric-8* is apparently also expressed in the embryo; however, we have not yet determined whether embryonically expressed *ric-8* is important only for early embryogenesis or whether it also functions at later stages.

GOA-1 ($G_o\alpha$) and RIC-8 are required for centrosomal rocking in one-cell embryos: To investigate the cause of the embryogenesis defect, we used Nomarski optics to observe wild-type and mutant embryos as they developed from single cells to the eight-cell stage. Many of the earliest events that occur in the one-cell embryo after fertilization occurred normally in *goa-1* and *ric-8* mutant embryos. In observations of multiple embryos from each mutant (at least eight embryos each from *goa-1(pk62)*, *ric-8(md303)*, and embryos derived from *goa-1/+; ric-8/ric-8* parents) polar body extrusion, anterior membrane contractions, pseudocleavage, and the migration, fusion, and rotation of the two pronuclei, were not obviously different from wild-type embryos with respect to appearance, timing, or location of the events (data not shown; see Strome and Wood 1983; and Albertson 1984 for a description of these events). This suggests that the microtubule- and microfilament-based cytoskeletons are not significantly disrupted in *ric-8* and *goa-1* mutants, since a previous study found that pronuclear migration requires an intact microtubule cytoskeleton, and that pseudocleavage and pronuclear rotation require an intact microfilament cytoskeleton (Strome and Wood 1983).

After these early events the first mitotic spindle forms and, during its formation, the posterior centrosome rocks back and forth, crossing the midline of the embryo at least four to six times (Strome and Wood 1983; Albertson 1984; K. G. Miller, unpublished observations). The rocking is accompanied by posterior movement of the centrosome. This results in the mitotic spindle being positioned more toward the posterior end of the embryo, and subsequent cleavage then results in a larger anterior AB cell and a smaller posterior P_1 cell. We observed that one-cell posterior centrosome rocking was weak or absent in *ric-8(md303)* mutant embryos and was absent altogether in embryos derived from *goa-1/+; ric-8/ric-8* parents. The centrosomal rocking was present in *goa-1(pk62)* mutant embryos, but appeared less pronounced (data not shown). The posterior centrosome still appeared to move posteriorly in embryos derived from *goa-1/+; ric-8/ric-8*; however, the final position of the spindle in these mutants was often less posterior than in the wild type, which often resulted in an AB blastomere that was only slightly bigger than the P_1 blastomere or, less often, blastomeres of equal size (Figures 1, C and D, 3C, and 4, J and K). Although a function for one-cell posterior centrosomal rocking has not been described previously, our results indicate that this event may be important for establishing the size asymmetry between AB and P_1. Perhaps as an indirect consequence of the disruption of centrosomal rocking, the time required for progression from pronuclear fusion through the first cleavage was longer than wild type in all three

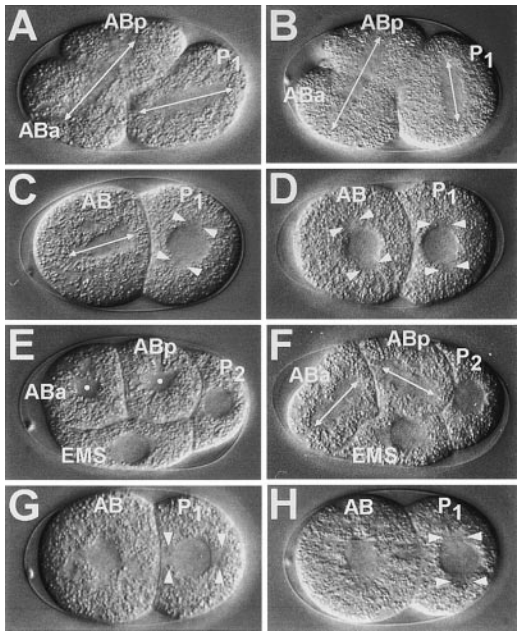

FIGURE 1.—Spindle alignment defects in *ric-8* and *goa-1* mutants. Anterior is left, and dorsal is up. *C. elegans* embryos are ~50 μm along the long axis. (A) Wild-type embryo at the late two-cell/early three-cell stage. Arrows indicate the orientation of the mitotic spindles, which are visible as cytoplasm free of yolk granules. The AB cell is undergoing cytokinesis, which will give rise to the cells ABa and ABp. The AB spindle was initially oriented dorsal-ventral, but has skewed to anterior-ventral/posterior-dorsal, as the elongating P_1 cell spindle forces ABa against the curved eggshell. Note that the orientation of the P_1 spindle is anterior-posterior. (B) A *ric-8* embryo at the three-cell stage. Note that the P_1 spindle is forming in a roughly dorsal-ventral orientation. This was the result of failed rotation of the P_1 centrosome-nucleus complex. (C and D) Two-cell embryos derived from *goa-1/+; ric-8/ric-8* parents. In C the AB spindle is forming in a roughly anterior-posterior orientation instead of the expected dorsal-ventral orientation. The far anterior end of the spindle is below the plane of focus. Also note the position of the two P_1 centrosomes (each centrosome is between a pair of arrowheads), which are not oriented anterior-posterior as they should be at this stage. In D the AB centrosomes (arrowheads) are tilted ~20° counterclockwise of the proper dorsal-ventral orientation. Such skewing does not normally occur until the P_1 spindle axis forms (see A). The P_1 centrosomes are visible on the dorsal and ventral side of the nucleus (arrowheads). (E) Wild-type embryo at the late four-cell stage. The ABa and ABp spindles are forming in the proper left-right (or *z*-) axis and are visible in cross-section (indicated by white dots). (F) Embryo derived from a *goa-1/+; ric-8/ric-8* parent. Note that the ABa spindle is oriented anterior-ventral/posterior-dorsal and the ABp spindle is oriented roughly anterior-posterior. (G) Wild-type embryo at the two-cell stage. Each set of arrowheads in the P_1 cell points to a centrosome, which are visible as smooth knobs on opposite sides of the nucleus. Note that at this time (9.8 min after the birth of P_1), the wild-type centrosomes are in an anterior-posterior orientation, which will be the future orientation of the mitotic spindle. This orientation resulted from a 90° rotation of the centrosome-nucleus complex. (H) *goa-1(pk62)* mutant embryo at the two-cell stage, 12.4 min after the birth of P_1. Note that the P_1 centrosomes are still oriented dorsal-ventral. The centrosome-nucleus complex of this cell later rotated partly (~45°) and the spindle orientation was further corrected to anterior-posterior during anaphase. Note that the AB spindle is beginning to form in the correct dorsal-ventral orientation.

mutant strains. The time differences amounted to 10–16%, depending on the strain, and were statistically significant. We also measured the time required for wild-type and mutant embryos to progress through the first two cycles of cell division (from P_1 telophase to P_3 telophase), and we observed that embryos derived from *goa-1(n1134)/+; ric-8(md303)*, *ric-8(md303)*, and *goa-1(pk62)* took, on average, 10, 12, and 18% longer than wild-type embryos, respectively. We found the increased cell cycle times to be statistically significant (*t*-test *P* values ≤ 0.004); however, given the nature of the gene products, it seems likely that this small effect on cell cycle times is an indirect, rather than primary, effect of the mutations.

GOA-1 ($G_o\alpha$) and RIC-8 are required for mitotic spindle alignment in early embryogenesis: In wild-type young embryos, the mitotic spindle of each cell assumes a stereotypical alignment that determines the cleavage plane axis at cytokinesis (SULSTON *et al.* 1983). This ensures that the cells have a fixed position with respect to each other. The first zygotic cell, P_0, divides along the anterior-posterior axis to produce AB and P_1. AB then divides along the dorsal-ventral axis to produce ABa and ABp, and P_1 divides along the anterior-posterior axis to produce EMS and P_2 (SULSTON *et al.* 1983).

We observed that a significant fraction of the mitotic spindles in *ric-8(md303)* embryos were misaligned, which sometimes resulted in an altered arrangement of cells (Figure 1B; Table 2). Not all of the cells, however, appeared equally susceptible to spindle misalignments. For example, the P_0 spindle was only misaligned in 1 of 16 embryos, and the EMS and P_2 spindles were only misaligned in 2 of 14 embryos. The spindles of AB, P_1, ABa, and ABp, however, were misaligned in ~30–50% of *ric-8* embryos (Table 2). Some of these misalignments, particularly those of the P_0 and P_1 spindles, were eventually corrected to the wild-type alignment during anaphase. In those cells with misaligned spindles, the spindle orientation, in general, appeared random and frequently deviated from the wild-type orientation by 25–90° (Table 3; data not shown). The misalignment of P_1 cell spindles, however, was not random. In wild-type P_1 cells, the centrosome-nucleus undergoes a 90° rotation that changes the alignment of the two opposed centrosomes from dorsal-ventral to anterior-posterior (HYMAN and WHITE 1987). In *ric-8* embryos, this rotation often occurs only partially or fails completely. Since the P_1 centrosomes determine the spindle alignment (HYMAN and WHITE 1987), the P_1 cell spindles of *ric-8* embryos are often oriented in planes with a significant dorsal-ventral component (Figure 1B; Table 3).

Consistent with the high rate of embryonic lethality that we observed in embryos derived from *goa-1/+; ric-8/ric-8* parents, we also observed a striking increase in mitotic spindle misalignments in these embryos relative to *ric-8* and *goa-1* single mutants (Figure 1, C, D, and F; Table 2). As we observed for *ric-8* single mutants, not all of the cells were equally susceptible to the misalign-

TABLE 2

GOA-1 and RIC-8 are required for proper mitotic spindle alignment in early embryogenesis

	Cell						
Parental genotype	P_0	AB	P_1	ABa	ABp	EMS	P_2
Wild type	0/25	0/25	0/25	0/25	0/25	0/25	0/25
ric-8(md1712 md303)[a]	0/3	0/3	0/3	0/3	0/3	0/3	0/3
ric-8(md303)	1/16[b]	5/16	9/16[c]	7/16	6/16	2/14	2/14
goa-1(pk62)	0/10	0/10	5/10[d]	1/10	0/10	0/10	0/9
goa-1(n1134)/+; ric-8(md303)	2/24[e]	16/24	24/24	18/20	19/20	5/20	9/20

Shown is the fraction of embryos showing a misaligned mitotic spindle for each cell at the stage of mitotic prometaphase (the denominator equals the total number of embryos examined for a particular cell). We define "misaligned mitotic spindle" as a spindle that is at least 30°–45° off from the wild-type alignment.

[a] Intragenic revertant that suppresses the *md303* mutant phenotypes; used here as a control.

[b] The misaligned spindle was corrected during anaphase.

[c] Four of the nine misaligned spindles were corrected during anaphase.

[d] Four of the five misaligned spindles were corrected to anterior-posterior during anaphase.

[e] Both of the misaligned spindles were corrected during anaphase.

ments. The P_0 spindle was misaligned in only 2 of 24 embryos. In contrast, P_1, ABa, and ABp spindles were misaligned in 90–100% of embryos, while AB, EMS, and P_2 spindles were misaligned in 66, 25, and 45% of embryos, respectively (Table 2). In those cells with misaligned spindles, the spindle orientation appeared random, with the exception of the P_1 cell (Table 2). As we observed for *ric-8* single mutants, the misaligned P_1 spindles coincided with a partial or complete failure of the rotation of the centrosome-nucleus complex, which resulted in spindle orientations with a significant dorsal-ventral component (Figure 1, C and D; Table 3). The spindle misalignments in the AB cell lineage also appeared to be a consequence of improper centrosome position at the time of mitotic spindle formation (Figure 1D).

In contrast to *ric-8* mutant embryos, most of the mitotic spindles of *goa-1* single-mutant embryos exhibited wild-type alignments. The exception was the P_1 cell, which, as we observed for *ric-8(md303)*, failed partially or completely in the rotation of the centrosome-nucleus complex in 5 out of 10 embryos (Figure 1H; Table 2).

Why were P_0, EMS, and P_2 less susceptible to spindle misalignments? In P_0, pronuclear migration, fusion, and rotation occur normally in the mutants. Therefore, these early events, which probably determine spindle alignment in P_0, seem to have less of a requirement for GOA-1 and RIC-8. EMS may be less susceptible to spindle misalignment because it is a long, narrow cell, and the normal alignment of its mitotic spindle is along its long axis. A recent study suggests that incorrectly aligned EMS spindles may rotate passively to the correct orientation as a consequence of the cell's shape (Schlesinger *et al.* 1999). Our data, therefore, probably do not accurately reflect the true extent of EMS spindle misalignments. Finally, the P_2 cell is also unique because, during prophase, its nucleus undergoes stereotyped movements along the membrane segments that border the ABp and EMS cells (described below), which could potentially affect or bias spindle alignment.

The spindle alignment defects are unlikely to be a consequence of perturbed embryonic polarity, as is the case with the *par* mutants. In general, embryos from *par* mothers undergo a symmetric first division, followed by synchronous subsequent divisions that often exhibit

TABLE 3

Examples of spindle orientations in embryos derived from *ric-8(md303)* and *goa-1/+; ric-8/ric-8*

Cell	AB	P_1	ABp
A. Embryos derived from *ric-8/ric-8*			
Wild type	d/v	a/p	l/r
Mutant 1	dr/vl	d/v	vl/dr
Mutant 2	d/v	d/v	av/pd
Mutant 3	d/v	dr/vl	l/r
Mutant 4	d/v	a/p	l/r
Mutant 5	dl/vr	a/p	dl/vr
Mutant 6	av/pd	a/p	l/r
Mutant 7	d/v	d/v	dr/vl
Mutant 8	d/v	d/v[a]	l/r
B. Embryos derived from *goa-1/+; ric-8/ric-8*			
Wild type	d/v	a/p	l/r
Mutant 1	d/v	d/v	al/pr
Mutant 2	dr/vl	ad/pv	dl/vr
Mutant 3	dl/vr	dr/vl	dr/vl
Mutant 4	d/v	d/v	d/v
Mutant 5	av/pd	d/v	a/p
Mutant 6	ad/pv	dr/vl	d/v
Mutant 7	al/pr	av/pd	d/v
Mutant 8	d/v	dr/vl	ar/pl

Shown are the spindle orientations (estimated to the nearest 45°) for three cells (AB, P_1, and ABp) in eight representative embryos for each mutant genotype. a, anterior; p, posterior; d, dorsal; v, ventral; l, left; r, right.

[a] Cleavage plane was corrected to a/p before cytokinesis.

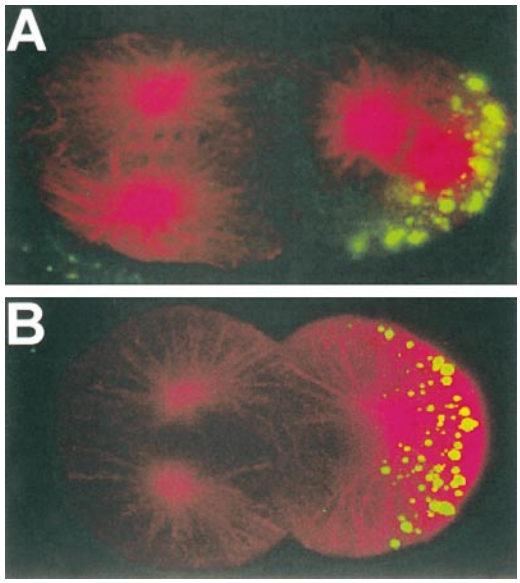

FIGURE 2.—P granules are normally localized in embryos derived from *goa-1/+; ric-8/ric-8*. Anterior is left, and dorsal is up. (A) Two-cell wild-type embryo stained with antibodies to PGL-1 (green) and tubulin (red). PGL-1 is a component of the P granules (KAWASAKI *et al.* 1998). Note that the P granules are localized to the posterior end of the P_1 cell. This localization pattern is essentially unchanged in embryos derived from a *goa-1/ +; ric-8/ric-8* parent (B). Also note that microtubules in the mutant embryo (B), before centrosome replication (right cell, P_1) and after centrosome replication (left cell, AB), appear to extend properly from the centrosomes to the plasma membrane.

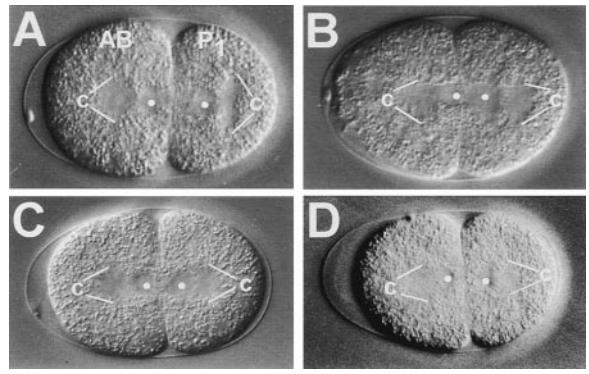

FIGURE 3.—*goa-1* and *ric-8* mutant embryos exhibit defective P_1 centrosome flattening. Anterior is left. *C. elegans* embryos are ~50 μm along the long axis. (A) Wild-type two-cell embryo at 5 sec after the completion of P_0 cleavage. The centers of the newly forming nuclei are indicated with white dots. Each pair of white lines marked with a c indicates the location of a centrosome that, before cleavage, formed one end of the mitotic spindle. The astral microtubule arrays around the centrosomes, like the nuclei, are visible as areas that are largely devoid of yolk granules. Note that the P_1 centrosome has flattened into a disc that appears as a line in the plane of focus. (B–D) Two-cell embryos derived from *goa-1(pk62)* (B), *goa-1(n1134)/+; ric-8(md303)/ric-8(md303)* (C), and *ric-8(md303)* (D) at $t = 0$ sec, $t = 18$ sec, and $t = 15$ sec after the completion of P_0 cleavage, respectively. Note that the P_1 centrosome (c) in all three mutant strains is roughly circular in cross-section, rather than long and narrow like wild-type P_1 centrosomes.

mitotic spindle misalignments. In addition, *par* embryos show missegregation or no segregation of P granules (KEMPHUES *et al.* 1988). In contrast to *par* embryos, we found that, as in wild-type embryos, in all three types of mutant embryos (*goa-1*, *ric-8*, and embryos derived from *goa-1/+; ric-8/ric-8*), the P_1 cell divided after its AB sibling and the P_2 cell divided after its EMS sibling (data not shown). Second, we observed that germline P granules, which in wild type are segregated at each cell division to the germline precursor cell (STROME and WOOD 1983), are properly localized in embryos derived from *goa-1/+; ric-8/ric-8* (Figure 2). This suggests that the mitotic spindle misalignments are not associated with defects in overall embryonic polarity, as is the case with *par* embryos. In addition, since P-granule localization requires an intact actin cytoskeleton (STROME and WOOD 1983), these data provide further evidence that the actin cytoskeleton is intact in the mutants.

GOA-1 ($G_o\alpha$) and RIC-8 are required for P_1 centrosome flattening: During late telophase of the first cell cycle, the centrosome inherited by the P_1 cell exhibits a flattened morphology, which is in striking contrast to the roughly spherical centrosome in the AB cell (STROME and WOOD 1983; KEATING and WHITE 1988; Figure 3A). P_1 centrosome flattening is a relatively short-lived event, beginning at about the completion of cytokinesis and lasting only 1–2 min (K. G. MILLER, data not shown). We observed that embryos derived from *ric-8(md303)*, *goa-1(pk62)*, and *goa-1(n1134)/+; ric-8(md303)* exhibited roughly spherical P_1 centrosomes (Figure 3, B–D). RIC-8 and GOA-1, therefore, are required for P_1 centrosome flattening.

The effect of *ric-8* and *goa-1* mutations on centrosome morphology, however, seems to be restricted to the single telophase P_1 centrosome. The shape of the AB centrosome in these mutants appears indistinguishable from wild type (Figure 3). Furthermore, proper centrosome replication occurs in the mutant embryos and, as in wild type, daughter centrosomes become attached to, and migrate along, the nuclear membrane to become diametrically opposed (Figure 1, C, D, and H). In addition, the overall size and shape of the daughter centrosomes in both AB and P_1 cells does not appear different from the corresponding wild-type centrosomes (Figure 1, C, D, and H; K. G. MILLER, data not shown). Finally, immunofluorescence staining of tubulin in mutant embryos (embryos derived from *goa-1/+; ric-8/ric-8*) demonstrates that both pre- and postreplication centrosomes are capable of extending arrays of microtubules from the centriole cores to the plasma membrane (Figure 2B).

GOA-1 ($G_o\alpha$) and RIC-8 are required for proper nuclear migration in early embryogenesis: Because of the large size of early embryonic cells, proper positioning of nuclei is likely to be an important feature of early

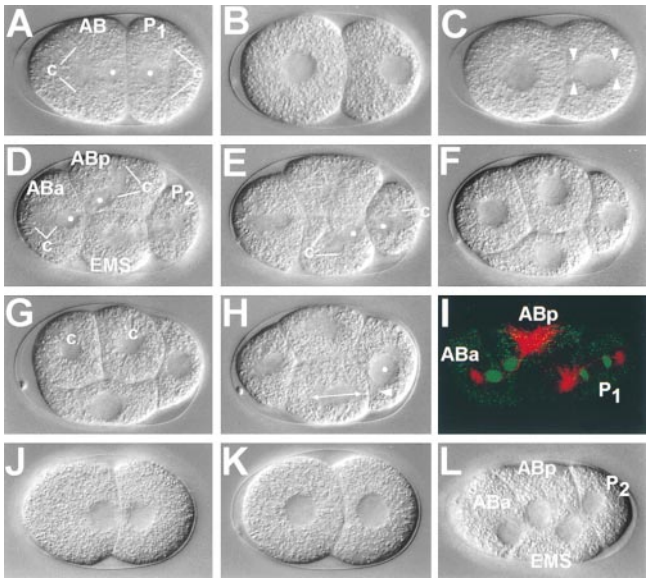

Figure 4.—Nuclear migration patterns in wild-type embryos and in embryos derived from *goa-1(n1134)/+; ric-8(md303)*. Anterior is left, and dorsal is up. (A–H) Key nuclear migration landmarks in wild-type two- and four-cell embryos. (A) Early wild-type two-cell embryo (1:10 min after cleavage of P_0). The white dots indicate the centers of the newly forming nuclei, which are very close to the cleavage membrane boundary. Each pair of white lines marked with a c indicates the location of a centrosome that, before cleavage, formed one end of the mitotic spindle. The astral microtubule arrays around the centrosomes, like the nuclei, are visible as areas that are largely devoid of yolk granules. Note that the P_1 centrosome has flattened into a disc that appears as a vertical line in the plane of focus. (B) Wild-type two-cell embryo at 6:00 min after cleavage. The nuclei have migrated outward from the cleavage membrane. The AB nucleus is roughly centered, while the P_1 nucleus is positioned in the far posterior part of the cell. (C) Wild-type two-cell embryo at 9:35 min after cleavage. The nucleus has now moved close to the AB cell membrane. The single centrosome has divided and the individual centrosomes have become associated with the nucleus. The centrosome-nucleus complex has rotated 90°. The individual centrosomes are visible as "knobs" that are devoid of yolk granules on either side of the nucleus (each pair of arrowheads points to a centrosome). The anterior centrosome appears to contact the AB cell membrane. (D) Early four-cell wild-type embryo (15:15 min after cleavage of P_0). The nuclei (indicated by white dots in each center) are again reforming very close to the cleavage membrane. Each centrosome (c) of the cleaved mitotic spindle is still visible. (E) The same four-cell wild-type embryo at 16:20 min after cleavage of P_0. This focal plane highlights the newly forming EMS and P2 nuclei (white dots in each center), which are reforming close to the cleavage boundary. Each centrosome (c) is indicated. (F) The same embryo (wild type) at 21:30 min after cleavage of P_0. Note that all four nuclei have moved away from their birth positions. The ABa, ABp, and EMS nuclei are approximately centered in the cell at this stage; however, at an earlier stage, the ABp nucleus normally occupies a more dorsal position in the cell before migrating back toward the cell center, and the ABa nucleus (also at earlier stage) normally moves slightly anterior of the center before moving back and occupying its present position. Note that the P_2 nucleus occupies a far posterior position in the cell at this stage. (G) The same embryo (wild type) at 24:55 min after cleavage of P_0. The mitotic spindles of ABa and ABp are forming in the left-right (*z*-) axis and the upper centrosome (c) of each spindle is visible in cross-section. The P_2 nucleus is now located close to the membrane boundary with ABp. (H) The same embryo (wild type) at 28:30 min after cleavage of P_0. The P_2 nucleus is now close to the EMS cell, where the mitotic spindle is forming (arrow), and its ventral centrosome (arrowhead) appears to make contact with the EMS-P_2 membrane boundary. (I) Wild-type three-cell embryo stained with an antibody to tubulin (red). DNA is stained with DAPI (green). At this stage, much of the tubulin staining is present in the asters of the recently cleaved ABa-ABp mitotic spindle and the not-yet-cleaved P_1 mitotic spindle. Note that the newly formed ABa and ABp nuclei (green) are positioned very close to the cleavage membrane boundary. (J) Two-cell embryo derived from *goa-1(n1134)/+; ric-8(md303)* 5:30 min after cleavage of P_0. Compare to wild type at a similar stage in B. Note that the two nuclei have not migrated significantly from their points of origin. (K) The same embryo shown in J at 9:00 min after cleavage of P_0. Note that the two nuclei are now positioned near the center of each cell. (L) Mutant embryo derived from a *goa-1(n1134)/+*; *ric-8(md303)* parent at 20:40 min after cleavage of P_0. All four nuclei are still near their points of origin. Compare to similar stage wild-type embryo in F.

development. However, surprisingly little is known about nuclear migration in early cellularized embryos, such as *C. elegans*, mouse, and human embryos. In Drosophila embryos, which are not cellularized until mitotic cycle 14, nuclei in the embryonic syncytium coordinately migrate to the embryo cortex at mitotic cycle 8 (Foe and Alberts 1983).

Using Nomarksi microscopy of developing embryos, we observed a stereotyped pattern of nuclear migrations in wild-type two- and four-cell embryos. In both two-cell and four-cell embryos, the sister nuclei reform at telophase close to the membrane boundary that was created by cytokinesis (Figure 4, A, D, and I). The nuclei then migrate outward on a vector toward the collapsing astral array of the inherited centrosome (Figure 4).

In two-cell embryos (Figure 4, A–C; Table 4) the AB nucleus continues migrating until it reaches a final position roughly in the cell center at an average of 6.5 min after telophase. The P_1 nucleus concomitantly migrates relatively rapidly to a position in the far posterior part of P_1, passing the center at an average of 2.8 min after telophase. The P_1 nucleus then migrates back toward the cell center, at which point the centrosome-nucleus rotation takes place. During rotation the nucleus moves slowly closer to the AB membrane boundary such that, at the end of the rotation, its anterior centrosome appears to contact the membrane boundary (Figure 4C).

In four-cell embryos (Figure 4, D–I; Table 4), ABa and ABp sister nuclei migrate outward and reach the cell center at an average of 5.3 min after cytokinesis. It is normal for both nuclei to move past their cell centers,

TABLE 4

GOA-1 and RIC-8 are required for proper nuclear migration in early embryogenesis

Genotype of parent	Cell				
	AB	P_1	ABa	EMS	P_2
N2 (wild type)	6.5 ± 0.2 (12/12)	2.8 ± 0.3 (12/12)	5.3 ± 0.3 (11/11)	5.2 ± 0.3 (11/11)	1.9 ± 0.9 (11/11)
ric-8(md303)	8.9 ± 0.5 (8/8)	7.2 ± 0.5 (8/8)	9.9 ± 0.9 (4/6)	8.3 ± 0.9 (5/6)	4.2 ± 0.4 (6/8)
goa-1(pk62)	8.3 ± 0.6 (9/9)	6.6 ± 0.6 (9/9)	7.3 ± 0.8 (9/9)	7.5 ± 1.2 (8/8)	3.0 ± 0.4 (6/7)
goa-1(n1134)/+; ric-8(md303)	8.8 ± 0.2 (8/9)	9.7 ± 0.8 (7/10)	— (0/7)	9.7 ± 1.2 (4/6)	— (0/7)

Times (in minutes) required for each nucleus to move from its position at telophase to an observer-defined position near the cell center. Values are mean ± standard error. Fractions below each number are the number of nuclei that achieved a position near the cell center over the total number examined. The numerator is the sample size from which the nuclear positioning times were calculated. Values for ABp nuclei are not shown, but are not significantly different from ABa nuclei. The nuclear migration time for the EMS cell in *goa-1(pk62)* is not significantly different from that of wild type. All other times are significantly greater than in wild type. The *t*-test *P* values are ≤0.015 for *goa-1(pk62)*, ≤0.002 for *ric-8(md303)*, and ≤0.000 for *goa-1(n1134)/+; ric-8(md303)*. Nuclear migration times for *goa-1(pk62)* are not significantly different than those for *ric-8(md303)*. The *t*-test *P* values are ≥0.072 for ABa and P_2 and ≥0.406 for AB, P_1, and EMS.

with ABa reaching a slightly anterior position and ABp often reaching a significantly dorsal position in the cell; however, both nuclei move back more toward the cell center shortly thereafter (Figure 4F). Cytokinesis of P_1 and the subsequent migrations of the EMS and P_2 nuclei occur ~1 min after the corresponding AB events. The EMS nucleus slowly migrates outward to reach a position near the cell center at an average of 5.2 min after cytokinesis. However, by the point at which ABa and ABp enter metaphase and begin dividing, the EMS nucleus is positioned near the ventral membrane (Figure 4G), although it is still roughly centered in the anterior-posterior axis. Like P_1, the P_2 nucleus moves rapidly out to a position at the far posterior of the cell (Figure 4F), passing the cell center at an average of 1.9 min after cytokinesis. By the time ABa and ABp enter metaphase, however, the P_2 nucleus is positioned very close to the ABp membrane boundary (Figure 4G). The P_2 nucleus then moves ventrally along the ABp membrane boundary until, at the point at which the EMS cell enters metaphase, the P_2 nucleus is positioned close to the EMS membrane boundary, such that its ventral centrosome appears to contact the membrane (Figure 4H).

These migrations were essentially invariant among 25/25 wild-type embryos that we examined. In two- and four-cell embryos from all three mutant strains, however, we observed that these migrations were delayed or, in some cases, did not occur properly. In *ric-8* and *goa-1* embryonic cells the nuclei remain near their points of origin for abnormally long times before slowly migrating outward. When we compared the time needed for nuclei from wild-type and mutant embryos to reach a position near the cell center, we found that *ric-8(md303)* nuclei took 1.4 to 2.5 times as long as wild type, and indeed 5 of 36 nuclei were unable to reach the cell center before the prometaphase stage, when the nuclear envelope breaks down (Table 4). *goa-1(pk62)* nuclei also migrated significantly slower than the wild type, although only 1 of 42 nuclei did not reach the cell center (Table 4). As noted previously, however, the most dramatic of all early nuclear migrations, pronuclear migration, occurred normally in all three mutant strains.

Consistent with our studies of embryonic lethality and spindle alignment, we observed an enhancement of the nuclear migration defect in embryos derived from *goa-1/+; ric-8/ric-8* parents. Examples of nuclear migration defects in these embryos are shown in Figure 4, J–L. The long nuclear migration times of these embryos resulted in a greater number of nuclei that did not reach the cell center before nuclear envelope breakdown (Table 4). This is most evident in the ABa, ABp, and P_2 cells, in which no nuclei reached the cell center. In contrast, however, most nuclei from the AB, P_1, and EMS cells did eventually reach the cell center (Figure 4, J and K; Table 4).

Since interphase nuclear migration happens before mitotic spindle alignment, we looked for evidence that the delayed nuclear migration might be causing spindle misalignments. We did this by comparing nuclear migration times with spindle alignment data in specific cells and mutants. The enhancement of both nuclear migration time and spindle misalignments in embryos derived from *goa-1/+; ric-8/ric-8* is consistent with delayed nuclear migration causing spindle misalignments. Other

data, however, argue against this hypothesis. For example, AB nuclear migration times were the same in *ric-8* embryos and in embryos derived from *goa-1/+; ric-8/ric-8*, and yet AB cells from *goa-1/+; ric-8/ric-8* were more than twice as likely to have a misaligned spindle (compare Tables 2 and 4). Similarly, the nuclear migration times in the cells of *goa-1(pk62)* embryos were not significantly different from those of *ric-8(md303)* embryos, and yet spindle misalignments were much more frequent in *ric-8(md303)* embryos (compare Tables 2 and 4). These results suggest, therefore, that delayed nuclear migration, of the scope we observed, is not sufficient to cause mitotic spindle misalignment.

We also observed that, although the rate of nuclear migration was slowed in the mutant strains, the direction of migration, once it occurred, was the same as in the wild type (*i.e.*, outward on a vector toward the collapsing astral array). This suggests that the basic cytoskeletal machinery that mediates nuclear movement in these mutants is intact.

GOA-1 ($G_o\alpha$) is localized to the cell cortex and to centrosomes in embryos and is concentrated in neuronal processes in the adult nervous system: We used immunofluorescence to determine the localization of GOA-1 in early embryonic cells. We observed that GOA-1 is concentrated intracellularly, at the cell cortices (Figure 5, A and C). The staining appeared brightest near regions of the cell membrane that contact other cells, with lighter staining near cell membrane regions that do not contact other cells. However, some or all of the brighter staining at shared membrane boundaries may simply be the result of having two juxtaposed membranes. We also observed a faint cloud of staining around the centrosomes (Figure 5, A and B). Both the cell cortex staining and the centrosomal staining is reduced, but not eliminated, in *goa-1(n363)* mutants (Figure 5D). This cell cortex and centrosomal staining pattern is strikingly similar to that described for GPB-1 (Gβ; Zwaal *et al.* 1996).

In adult animals, however, GOA-1 was no longer detectable in all cells, but instead was concentrated throughout the nervous system (Figure 5E). GOA-1 was most concentrated in neuronal processes; however, we also detected lighter staining in neuronal cell somas. As we observed for the embryonic staining, neuronal GOA-1 staining was strongly reduced, but not eliminated, in *goa-1(n363)* mutants (Figure 5F). The localization of GOA-1 to both embryonic and neuronal cells supports our findings that GOA-1 functions in both cell types.

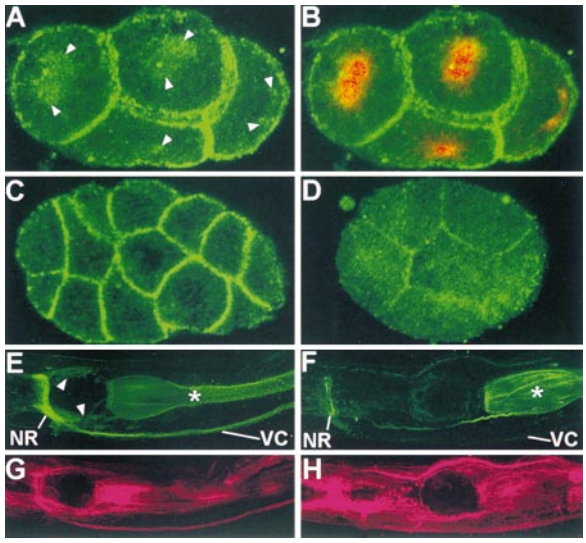

Figure 5.—GOA-1 localization in embryos and adults. (A and B) Wild-type four-cell embryo stained with an antibody to GOA-1 (green staining). In (B) the same embryo is shown overlaid with tubulin staining (red). Note that GOA-1 immunoreactivity is most concentrated near regions of the cell membrane that contact other cells. Lighter staining is also seen in cell membrane regions that do not contact other cells as well in regions around the centrosomes (arrowheads in A; compare with tubulin staining in B). (C) Single confocal plane of a ~20-cell wild-type embryo stained with the GOA-1 antibody, showing that GOA-1 staining is most concentrated near regions of the cell membrane that contact other cells. (D) Single confocal plane of an approximately six-cell *goa-1(n363)* loss-of-function mutant embryo stained with antibodies to GOA-1 (green staining). GOA-1 staining is strongly reduced and diffuse. (E and F) Wild-type (E) and *goa-1(n363)* (F) adults stained with the antibody to GOA-1 (green staining). In wild-type worms (E), GOA-1 is concentrated in the neuronal processes of the nerve ring (NR) and ventral nerve cord (VC). Arrowheads indicate neuronal cell somas, where lighter staining can also be seen. The asterisk indicates nonspecific staining of the gut, which is not diminished in the mutant. The neuronal staining is diminished in the mutant. (G and H) The same animals stained with a mixture of antibodies to CHA-1 and tubulin (both are shown as red staining) to control for permeabilization.

DISCUSSION

GOA-1, RIC-8, and centrosomes: Our findings show that GOA-1 and RIC-8 are required for multiple events during early embryogenesis. Although all of the events that are affected in *goa-1* and *ric-8* mutants rely on an intact cytoskeleton, the microfilament and microtubule cytoskeletons are intact and functional in the mutants, and embryonic polarity appears unperturbed. The common denominator of the mutant phenotypes appears to be a disruption of events that involve centrosomes; however, the centrosomes themselves, with the exception of the telophase P_1 centrosome (discussed below), appear unperturbed. The centrosomes of the mutant embryos replicate normally and appear to have normal size and shape (with the exception of the P_1 telophase centrosome). Daughter centrosomes exhibit diametric movements along the nuclear membrane, and both pre- and postreplicated centrosomes extend microtubules properly to the plasma membrane and along nor-

mal-size mitotic spindles. Three of the four mutant phenotypes, however, appear to result from defects in centrosomal movements (absence of one-cell posterior centrosome rocking, mitotic spindle misalignment, and delayed nuclear migration). Since centrosomal movements occur through microtubules and microtubule motors (Hyman 1989; see Morris *et al.* 1995; Skop and White 1998; Heil-Chapdelaine *et al.* 1999; Karki and Holzbaur 1999 for references), we hypothesize that the defects we observed may be the result of a breakdown in the signals that control the localization or localized activation of a specialized subset of microtubules, microtubule capture proteins, or microtubule motors. One possibility is that GOA-1 ($G_o\alpha$) and/ or GPB-1 ($G\beta$) interact directly with tubulin and/or microtubules. Previous studies have found that several G protein α subunits, including $G_o\alpha$, can activate the GTPase activity of tubulin and inhibit microtubule assembly (Wang and Rasenick 1991; Roychowdhury *et al.* 1999), while a $G\beta\gamma$ complex ($\beta_{1\gamma 2}$) was found to promote microtubule assembly (Roychowdhury and Rasenick 1997). Although intriguing, further investigation will be necessary to determine whether or not these interactions reflect the *in vivo* roles of GOA-1 ($G_o\alpha$) and/or GPB-1 ($G\beta$) in embryos.

Given that three of the mutant phenotypes involve centrosomal movements, it seems likely that the fourth phenotype, P_1 centrosome flattening, might reflect a defect in the interaction between the centrosome and one or more subsets of microtubules. Indeed, a recent study found that centrosome flattening was temporally correlated with the selective depletion of microtubules at the posterior of P_1 (Keating and White 1998). The action of a centrosome-based microtubule motor on a subset of unanchored microtubules is one of the possible explanations that could account for this finding.

Signaling proteins that regulate centrosome movement: Although previous studies in *C. elegans* and in other organisms have begun to define the machinery that mediates centrosome movement (see the Introduction for references), much less is known about the signals that regulate centrosome movement. Our study is the first to show that a G protein signaling pathway regulates one-cell posterior centrosome rocking, P_1 centrosome flattening, and nuclear migration. A previous study identifying a role for $G\beta$ in mitotic spindle alignment was the first indication that a G protein signaling pathway is involved in that centrosome-controlled process (Zwaal *et al.* 1996); however, no previous study has identified a $G\alpha$ protein that is involved in mitotic spindle alignment. Since $G\beta$ mutants have more severe spindle alignment defects than *goa-1* loss-of-function mutants, however, it seems likely that at least one other $G\alpha$ protein also regulates mitotic spindle alignment. Since the entire set of 20 $G\alpha$-encoding *C. elegans* genes has now been identified (Jansen *et al.* 1999), it should be possible in future studies to identify which one(s) function with GOA-1 in mitotic spindle alignment.

What is the relationship of GOA-1 to RIC-8? Our finding that a 50% decrease in maternal *goa-1* gene dosage cannot support embryogenesis in backgrounds with reduced RIC-8 function suggests that the functions of GOA-1 and RIC-8 are closely linked. In the nervous system, RIC-8 and GOA-1 are both components of the $G_o\alpha$-$G_q\alpha$ signaling network (Miller *et al.* 2000). At two different points in the animal's life, therefore, the functions of RIC-8 and GOA-1 are closely associated. A closer analysis, however, reveals important and potentially informative differences between the two pathways. First, EGL-30 ($G_q\alpha$) appears not to play a role in the embryonic pathway (this study; K. G. Miller, data not shown). Second, in the embryonic pathway, reduction of function mutations in *goa-1* and *ric-8* lead to similar phenotypes that are enhanced in *goa-1/+; ric-8* double mutants, whereas in the adult neuronal pathway, the same *goa-1* and *ric-8* mutants have opposite phenotypes and suppress each other.

Another study suggests that RIC-8 plays a positive upstream role in EGL-30 ($G_q\alpha$) signaling in the nervous system (Miller *et al.* 2000); however, because EGL-30 ($G_q\alpha$) acts downstream of GOA-1 ($G_o\alpha$; Hajdu-Cronin *et al.* 1999; Miller *et al.* 1999), we cannot rule out the possibility that RIC-8 also has a positive role in GOA-1 ($G_o\alpha$) signaling in the nervous system. A positive role for RIC-8 in GOA-1 signaling in adults would be masked by RIC-8's effects on the downstream gene EGL-30. In the embryo, on the other hand, where EGL-30 apparently does not play a role, reducing RIC-8's function results in a *goa-1* reduction-of-function phenotype, which suggests that RIC-8 does play a positive role in GOA-1 ($G_o\alpha$) signaling in embryos. GPB-1 ($G\beta$) is one candidate for a molecule that is likely to be required for both EGL-30 ($G_q\alpha$) and GOA-1 ($G_o\alpha$) function and whose regulation by or of RIC-8 could account for our findings. GPB-1's role in mitotic spindle alignment during early embryogenesis, as well as locomotion and egg laying in adults, is consistent with this possibility (Zwaal *et al.* 1996).

What inputs regulate RIC-8-GOA-1 signaling? G proteins typically transduce signals from the plasma membrane to produce an intracellular response. Antibody localization studies are consistent with GOA-1 ($G_o\alpha$) and GPB-1 ($G\beta$) transducing signals from regions of the plasma membrane or cell cortex (this study; Zwaal *et al.* 1996). However, GOA-1 and GPB-1 also localize to centrosomes (Zwaal *et al.* 1996; this study). Therefore, although the GOA-1 and GPB-1 might be initially activated at the plasma membrane, they ultimately seem to interact with microtubules. It is tempting to speculate that, with respect to their mitotic spindle alignment functions, GOA-1, GPB-1, and RIC-8 may act downstream of intrinsic and/or extrinisic developmental

cues; however, further experiments will be necessary to determine whether or not this is the case.

We thank Michael Koelle, Susan Strome, and Janet Duerr for generously providing antibodies to GOA-1, PGL-1, and CHA-1, respectively. Confocal images were obtained in the Flow and Cytometry Laboratory in the Warren Medical Research Institute. Some of the strains used here were provided by the *Caenorhabditis elegans* Genetics Center. This work was supported by a grant from the National Institute of Neurological Disorders and Stroke to J.B.R. (NS33187).

LITERATURE CITED

Albertson, D. G., 1984 Formation of the first cleavage spindle in nematode embryos. Dev. Biol. **101:** 61–72.

Bowerman, B., 1998 Maternal control of pattern formation in early *Caenorhabditis elegans* embryos. Curr. Topics Dev. Biol. **39:** 75–117.

Brenner, S., 1974 The genetics of *C. elegans*. Genetics **77:** 71–94.

Brundage, L., L. Avery, A. Katz, U. Kim, J. E. Mendel *et al.*, 1996 Mutations in a *C. elegans* $G_q\alpha$ gene disrupt movement, egglaying and viability. Neuron **16:** 999–1009.

Duerr, J. S., D. L. Frisby, J. Gaskin, A. Duke, K. Asermely *et al.*, 1999 The *cat-1* gene *Caenorhabditis elegans* encodes a vesicular monoamine transporter required for specific monoamine-dependent behaviors. J. Neurosci. **19:** 72–84.

Foe, V. E., and B. M. Alberts, 1983 Studies of nuclear and cytoplasmic behavior during the five mitotic cycles that precede gastrulation in *Drosophila* embryogenesis. J. Cell Sci. **61:** 31–70.

Goldstein, B., 1995 Cell contacts orient some cell division axes in the *Caenhorabditis elegans* embryo. J. Cell Biol. **129:** 1071–1080.

Guo, S., and K. J. Kemphues, 1996 Molecular genetics of asymmetric cleavage in the early *Caenhorabditis elegans* embryo. Curr. Opin. Genet. Dev. **6:** 408–415.

Hajdu-Cronin, Y. M., W. J. Chen, G. Patikoglou, M. R. Koelle and P. W. Sternberg, 1999 Antagonism between $G_o\alpha$ and $G_q\alpha$ in *C. elegans*: the RGS protein EAT-16 is necessary for $G_o\alpha$ signaling and regulates $G_q\alpha$ activity. Genes Dev. **13:** 1780–1793.

Hawkins, N., and G. Garriga, 1998 Asymmetric cell division: from A to Z. Genes Dev. **12:** 3625–3638.

Heil-Chapdelaine, R. A., N. R. Adames and J. A. Cooper, 1999 Formin' the connection between microtubules and the cell cortex. J. Cell Biol. **144:** 809–811.

Hyman, A. A., 1989 Centrosome movement in the early divisions of *Caenhorabditis elegans*: a cortical site determining centrosome position. J. Cell Biol. **109:** 1185–1193.

Hyman, A. A., and J. G. White, 1987 Determination of the cell division axes in the early embryogenesis of *Caenhorabditis elegans*. J. Cell Biol. **105:** 2123–2135.

Jan, Y.-N., and L.-Y. Jan, 2000 Polarity in cell division: What frames thy fearful asymmetry? Cell **100:** 599–602.

Jansen, G., K. L. Thijssen, P. Werner, M. van der Horst, E. Hazendonk *et al.*, 1999 The complete family of genes encoding G proteins of *Caenhorabditis elegans*. Nat. Genet. **21:** 414–419.

Karki, S., and E. L. F. Holzbaur, 1999 Cytoplasmic dynein and dynactin in cell division and intracellular transport. Curr. Opin. Cell Biol. **11:** 45–53.

Kawasaki, I., Y.-H. Shim, J. Kirchner, J. Kaminker, W. B. Wood *et al.*, 1998 PGL-1, a predicted RNA-binding component of germ granules, is essential for fertility in *C. elegans*. Cell **94:** 635–645.

Keating, H. H., and J. G. White, 1998 Centrosome dynamics in early embryos of *Caenhorabditis elegans*. J. Cell Sci. **111:** 3027–3033.

Kemphues, K. J., J. R. Priess, D. G. Morton and N. S. Cheng, 1988 Identification of genes required for cytoplasmic localization in early *C. elegans* embryos. Cell **52:** 311–320.

Knoblich, J. A., 1997 Mechanisms of asymmetric cell division during animal development. Curr. Opin. Cell Biol. **9:** 833–841.

Lackner, M. R., S. J. Nurrish and J. M. Kaplan, 1999 Facilitation of synaptic transmission by EGL-30 $G_q\alpha$ and EGL-8 PLCβ: DAG binding to UNC-13 is required to stimulate acetylcholine release. Neuron **24:** 335–346.

Lee, L., J. S. Tirnauer, J. Li, S. C. Schuyler, J. Y. Liu and D. Pellman, 2000 Positioning of the mitotic spindle by a cortical-microtubule capture mechanism. Science **287:** 2260–2262.

Lu, B., L.-Y. Jan and Y.-N. Jan, 1998 Asymmetric cell division: lessons from flies and worms. Curr. Opin. Genet. Dev. **8:** 392–399.

Malone, C. J., W. D. Fixsen, H. R. Horvitz and M. Han, 1999 UNC-84 localizes to the nuclear envelope and is required for nuclear migration and anchoring during *C. elegans* development. Development **126:** 3171–3181.

Mendel, J. E., H. C. Korswagen, K. S. Liu, Y. M. Hajdu-Cronin, M. I. Simon *et al.*, 1995 Participation of the protein G_o in multiple aspects of behavior in *C. elegans*. Nature **267:** 1652–1655.

Miller, K. G., A. Alfonso, M. Nguyen, J. A. Crowell, C. D. Johnson *et al.*, 1996 A genetic selection for *Caenorhabditis elegans* synaptic transmission mutants. Proc. Natl. Acad. Sci. USA **93:** 12593–12598.

Miller, K. G., M. D. Emerson and J. B. Rand, 1999 $G_o\alpha$ and diacylglycerol kinase negatively regulate the $G_q\alpha$ pathway in *C. elegans*. Neuron **24:** 323–333.

Miller, K. G., M. D. Emerson, J. R. McManus and J. B. Rand, 2000 RIC-8 (Synembryn): a novel conserved protein that is required for $G_q\alpha$ signaling in the *C. elegans* nervous system. Neuron **27:** 289–299.

Morris, N. R., X. Xiang and S. M. Beckwith, 1995 Nuclear migration advances in fungi. Trends Cell Biol. **5:** 278–282.

Nurrish, S., L. Ségalat and J. M. Kaplan, 1999 Serotonin inhibition of synaptic transmission: $G\alpha_o$ decreases the abundance of UNC-13 at release sites. Neuron **24:** 231–242.

Raff, J. W., and D. M. Glover, 1989 Centrosomes, and not nuclei, initiate pole cell formation in *Drosophila* embryos. Cell **57:** 611–619.

Rappaport, R., 1996 *Cytokinesis in Animal Cells*. Cambridge University Press, Cambridge.

Roychowdhury, S., and M. M. Rasenick, 1997 G protein $\beta1\gamma2$ subunits promote microtubule assembly. J. Biol. Chem. **272:** 31576–31581.

Roychowdhury, S., D. Panda, L. Wilson and M. M. Rasenick, 1999 G protein α subunits activate tubulin GTPase and modulate microtubule polymerization dynamics. J. Biol. Chem. **274:** 13485–13490.

Schaefer, M., A. Shevchenko, A. Shevchenko and J. A. Knoblich, 2000 A protein complex containing Inscuteable and the Gα-binding protein Pins orients asymmetric cell divisions in *Drosophila*. Curr. Biol. **10:** 353–362.

Schlesinger, A., C. A. Shelton, J. N. Maloof, M. Meneghini and B. Bowerman, 1999 Wnt pathway components orient a mitotic spindle in the early *Caenorhabditis elegans* embryo without requiring gene transcription in the responding cell. Genes Dev. **13:** 2028–2038.

Ségalat, L., D. A. Elkes and J. M. Kaplan, 1995 Modulation of serotonin-controlled behaviors by G_o in *Caenhorabditis elegans*. Nature **267:** 1648–1651.

Seydoux, G., C. C. Mello, J. Pettitt, W. B. Wood, J. R. Priess *et al.*, 1996 Repression of gene expression in the embryonic germ lineage of *C. elegans*. Nature **382:** 713–716.

Skop, A. R., and J. G. White, 1998 The dynactin complex is required for cleavage plane specification in early *Caenhorabditis elegans* embryos. Curr. Biol. **8:** 1110–1116.

Strome, S., and W. B. Wood, 1983 Generation of asymmetry and segregation of germ-line granules in early *C. elegans* embryos. Cell **35:** 15–25.

Strome, S., P. Martin, E. Schierenberg and J. Paulsen, 1995 Transformation of the germ line into muscle in *mes-1* mutant embryos of *C. elegans*. Development **121:** 2961–2972.

Sulston, J., and J. Hodgkin, 1988 Methods, pp. 596–597 in *The Nematode Caenorhabditis elegans*, edited by W. B. Wood. Cold Spring Harbor Laboratory Press, Cold Spring Harbor, NY.

Sulston, J. E., E. Schierenberg, J. G. White and J. N. Thomson, 1983 The embryonic cell lineage of the nematode *Caenhorabditis elegans*. Dev. Biol. **100:** 64–119.

Wang, N., and M. M. Rasenick, 1991 Tubulin-G protein interactions involve microtubule polymerization domains. Biochemistry **30:** 10957–10965.

White, J., and S. Strome, 1996 Cleavage plane specification in *C. elegans*: how to divide the spoils. Cell **84:** 195–198.

Yu, F., X. Morin, Y. Cai, X. Yang and W. Chia, 2000 Analysis of *partner of inscuteable*, a novel player of *Drosophila* asymmetric divisions, reveals two distinct steps in inscuteable apical localization. Cell **100:** 399–409.

Zwaal, R. R., J. Ahringer, H. G. A. M. van Luenen, A. Rushforth, P. Anderson *et al.*, 1996 G proteins are required for spatial orientation of early cell cleavages in *C. elegans* embryos. Cell **86:** 619–629.

Communicating editor: R. K. Herman